Supporting Information for Casey M. Godwin*, Aubrey R. Lashaway, David C. Hietala, Phillip E. Savage, and Bradley J. Cardinale. "*Biodiversity improves the ecological design of sustainable biofuel systems*", Global Change Biology Bioenergy. *Corresponding Author.

Species selection. For each of the functions displayed in Fig. S1, we ranked each species composition relative to the others in the experiment. Ranks were assigned such that the best performer is rank 1 and the worst performer is rank 0. For each of the possible subsets of four species, we added together the performance ranks for all monocultures, two-species polycultures, and the four-species polyculture (see Experimental design). We then selected the combination of four species (A, B, D, and F) that exhibited the highest total ranks (Table S1). It is important to note that this species selection method does not necessarily optimize the chances of detecting overyielding or other effects of diversity. Indeed, the mean performance rank for the four-species polyculture ABDF itself was 0.46.

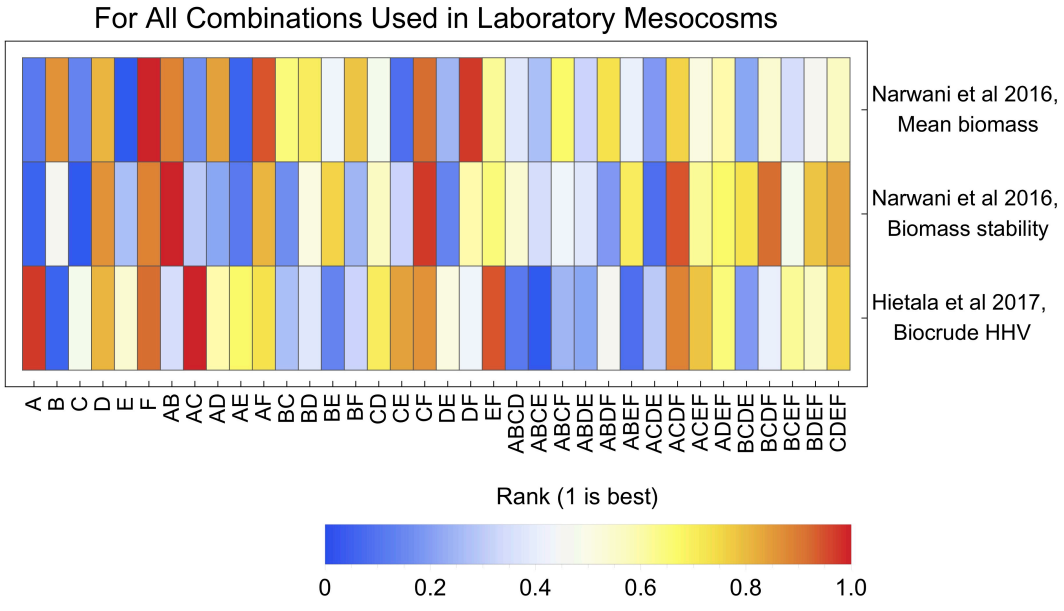

Supporting Information Fig. S1. Heatmap showing the performance rank of each species composition in previously published experiments (Hietala et al., 2017; Narwani, Lashaway,

Hietala, Savage, & Cardinale, 2016). Species codes are A=*Ankistrodesmus falcatus*, B=*Chlorella sorokiniana*, C=*Pediastrum duplex*, D=*Scenedesmus acuminatus*, E=*Scenedesmus ecornis*, F=*Selenastrum capricornutum*.

Mesocosms Mean Biomass,
Mesocosms Stability,
Biocrude HHV

4-Species Combination	Total Ranks For All Treatments
ABDF	20.51
ADEF	17.54
ABCF	17.24
BCDF	16.11
ACDF	15.97
BDEF	14.68
ABEF	14.46
CDEF	13.76
ABCD	13.24
BCEF	13.08
ACEF	12.89
ABDE	11.32
BCDE	8.03
ABCE	7.32
ACDE	6.76

Supporting Information Fig. S2. The four-species combination ABDF ranked highest and was selected for the present experiment. Species codes are A=*Ankistrodesmus falcatus*, B=*Chlorella sorokiniana*, C=*Pediastrum duplex*, D=*Scenedesmus acuminatus*, E=*Scenedesmus ecornis*, F=*Selenastrum capricornutum*.

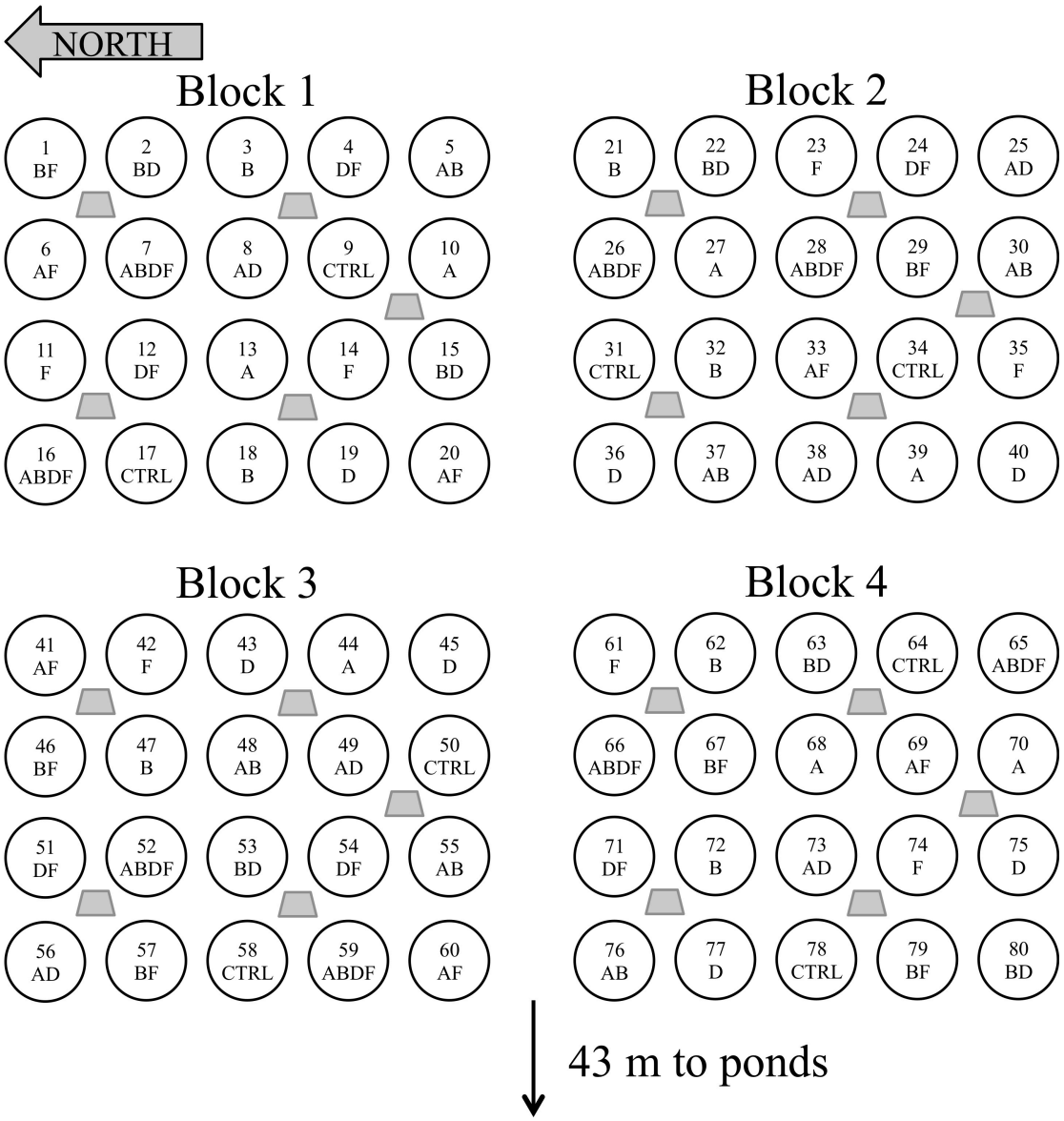

Supporting Information Fig. S3. Schematic diagram showing the spatial arrangement of the cattle tank ponds. Inset letter codes denote the inoculation treatments. Gray trapezoids represent air pumps (Pentair Aquatic Ecosystems, Pond Master AP-100) that supplied compressed air to groups of four ponds through vinyl tubing. Cattle tanks were 1.8 m in diameter, spaced 1 m apart within blocks, and blocks were separated by 3 m.

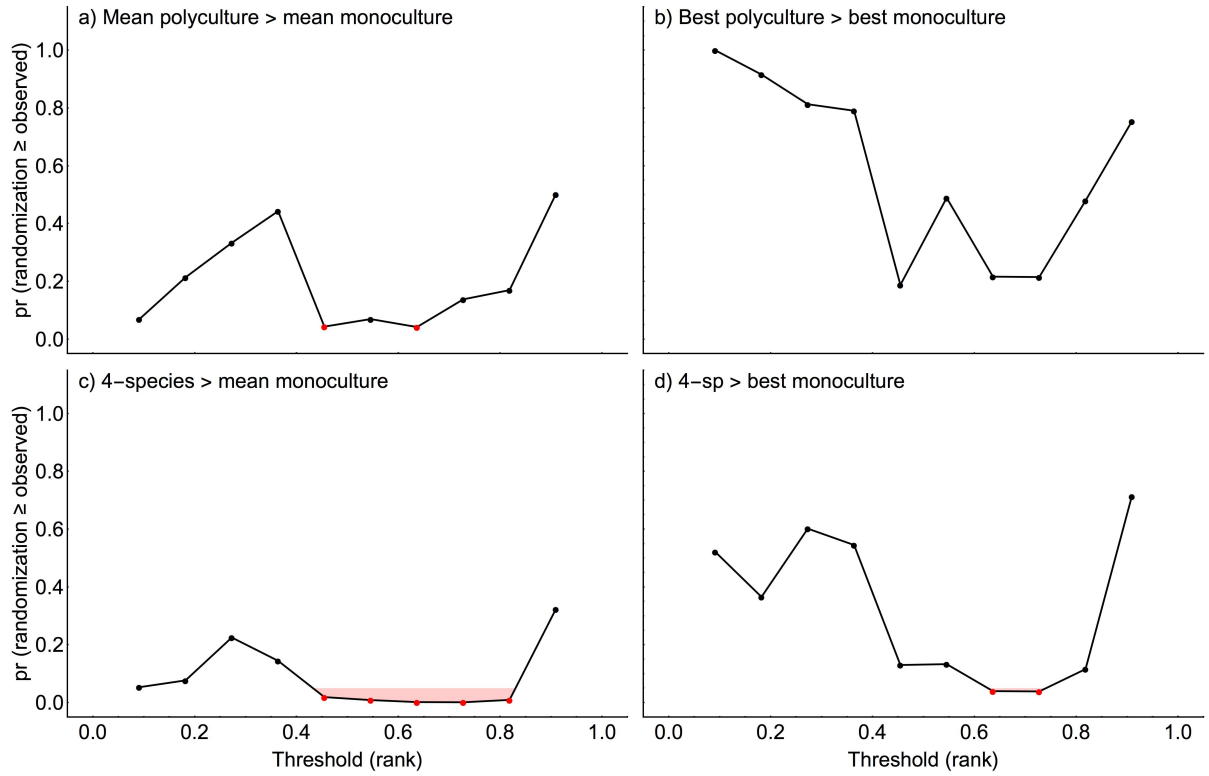

Supporting Information Fig. S4. Results of randomization tests comparing the multifunctionality of mono- versus polycultures. For each panel, we counted the number of functions performed above each threshold for mono- and polycultures, then compared the difference between those counts to the distribution of differences that resulted from randomizing the performance ranks. The horizontal axis displays the performance ranks and the vertical axis shows the proportion of iterations where the difference was equal to or greater than the observed difference (i.e. p-values). Red symbols are used to highlight observed differences that were greater than the 95th percentile of differences based on randomization (i.e. $p<0.05$).

Dissolved nutrients. We measured the concentrations of dissolved inorganic nutrients by centrifuging the cells and freezing the decanted supernatant at -20ºC. We measured soluble reactive phosphate using the ascorbic acid molybdenum method (American Public Health Association, 1995). We measured nitrate (nitrate + nitrite) using enzymatic conversion to nitrite (Nitrate Elimination Company, AtNAR-RPK), followed by the Naphthyl(ethylene)diamine dihydrochloride method (Ringuet, Sassano, & Johnson, 2011). Nitrate and phosphate measurements were referenced against a NIST-traceable standard (Hach Company). All water chemistry measurements were performed using a Biotek Synergy H1 plate reader.

There was no significant effect of species richness or species composition on nitrate concentration at week 5, but at week 10 the monoculture of *Selenastrum* (F) and polycultures dominated by *Selenastrum* (e.g. AF) had significantly higher amounts of nitrate remaining than the other treatments (Fig. S6, Table S1). Drawdown of phosphate was proportionally less than for nitrate and there was no significant effect of species richness at either week 5 or week 10.

Light attenuation. We measured attenuation of photosynthetically active radiation (PAR) by the cultures at weeks 5 and 10 using a spectrophotometric plate reader (Biotek Synergy H1). Samples and deionized water blanks were added to 48-well clear polystyrene microtiter plates and the absorbance was measured from 400 to 700 nm in 5 nm increments. For each wavelength, we used the water-corrected absorbance and the effective path length of 1.254 cm to estimate the extinction coefficient k (cm^{-1}) following Wetzel and Likens (2000). Because the spectrophometer does not measure light that is scattered by particles, but this light is still available for photosynthesis within the water column (Wetzel, 2001), we performed in-situ spectral analyses at week 10 to validate the spectrophotometer-derived estimates of k.

During full direct sunlight, we used a submersible spectrometer (Ocean Optics Jaz) to measure light intensity spectra at 0, 2, 4, 8, 16, and 32 cm. For all wavelengths and depths where there was detectable intensity, we computed the extinction coefficient k as the absolute value of the slope of log intensity versus depth. Three of the ponds did not yield complete in situ PAR spectra below 2 cm and thus did not provide reliable estimates of k at all wavelengths. The two methods for estimating k showed good correspondence when averaged across the entire PAR spectrum (r^2=0.88) or averaged across only the chlorophyll-a absorbance peaks at 430 to 450 nm (r^2=0.81) and 670 to 690 nm (r^2=0.82).

The species compositions differed substantially in terms of PAR light attenuation ($p<0.001$, Fig. S5). Ponds inoculated with *Selenastrum* (F) as a monoculture had significantly higher extinction coefficients than the other monocultures, resulting in a >95% attenuation of PAR within the first two centimeters of the water surface.

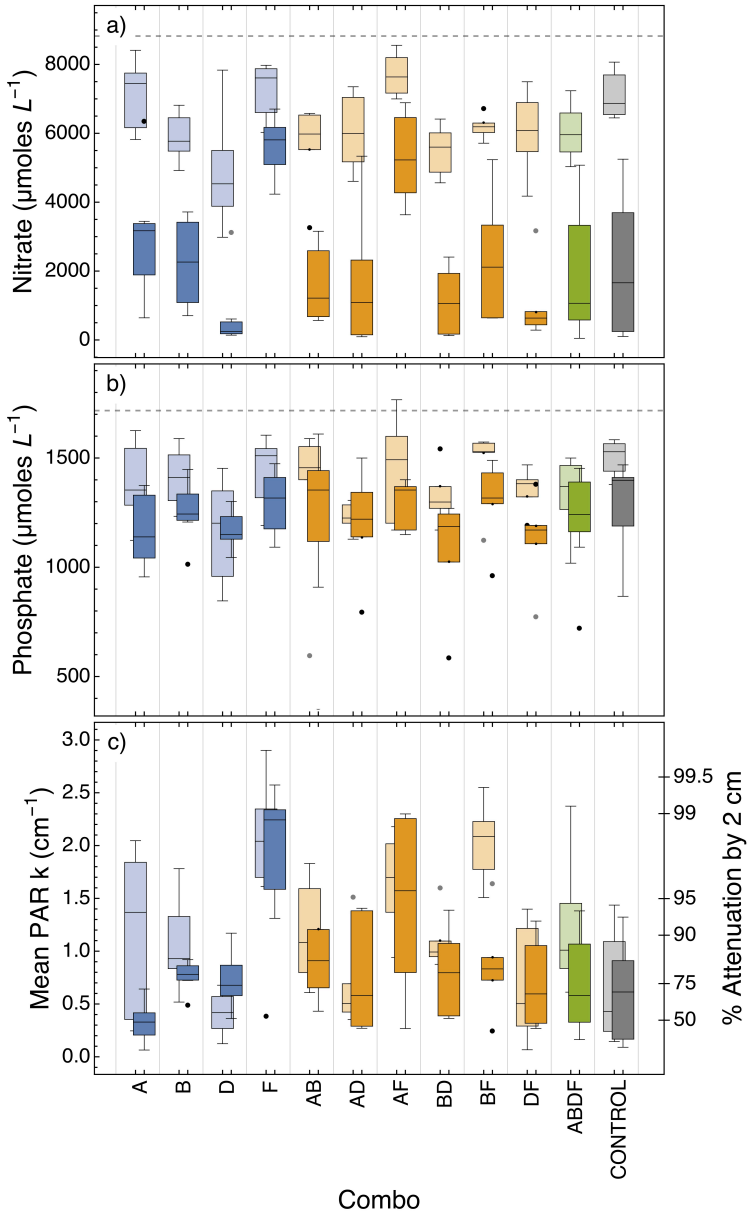

Supporting Information Fig. S5. Box-whisker charts showing the dissolved nitrate (A), dissolved phosphate (B), and PAR extinction coefficient (C) for replicate cattle tanks in each inoculation treatment. Light shading represents the values at week 5 and darker shading represents the values at week 10. Horizontal dashed lines denote the original nitrate and phosphate concentrations in the Bold-3N culture medium.

Table S1. Results of general linear models for nitrate concentration, phosphate concentration, and light attenuation coefficient. Effects of species combination (Combo) were nested in species richness (SR). Subscripts are used to display the numerator and denominator degrees of freedom (e.g. $F_{i,j}$). [b] Denotes spatial block was included as a random effect in the minimum adequate model and [p] denotes pond identity was included as a repeated measures random effect in the minimum adequate model.

Response variable	SR	SR|Combo	Time	SR*Time	Combo*Time
Nitrate [p]	$F_{2,75}$=0.64, p=0.53	$F_{8,75}$=0.87, p=0.55	$F_{1,43}$=690, $p<1x10^{-15}$	$F_{2,43}$=2.94, p=0.06	$F_{8,43}$=4.8, p<0.001
Phosphate	$F_{2,132}$=0.03, p=0.97	$F_{8,132}$=2.63, p<0.02	$F_{1,132}$=18.9, p<0.001	$F_{2,122}$=0.04, p=0.96	$F_{8,122}$=0.78, p=0.62
PAR (k) [b,p]	$F_{2,61}$=0.35, p=0.71	$F_{8,61}$=4.11, p<0.001	$F_{1,61}$=9.97, p<0.01	$F_{2,61}$=0.72, p=0.49	$F_{10,61}$=2.54, p<0.02

Water temperature. Temperature recorders were deployed in one pond within each block for the duration of the experiment (Hobo, Onset Computer Corporation). Air temperatures were obtained from a weather station located 18 km of the reserve. Pond temperature varied less than air temperature and ponds were generally within ±1ºC of each other. Temperature variation over the course of the experiment is summarized in Fig. S6.

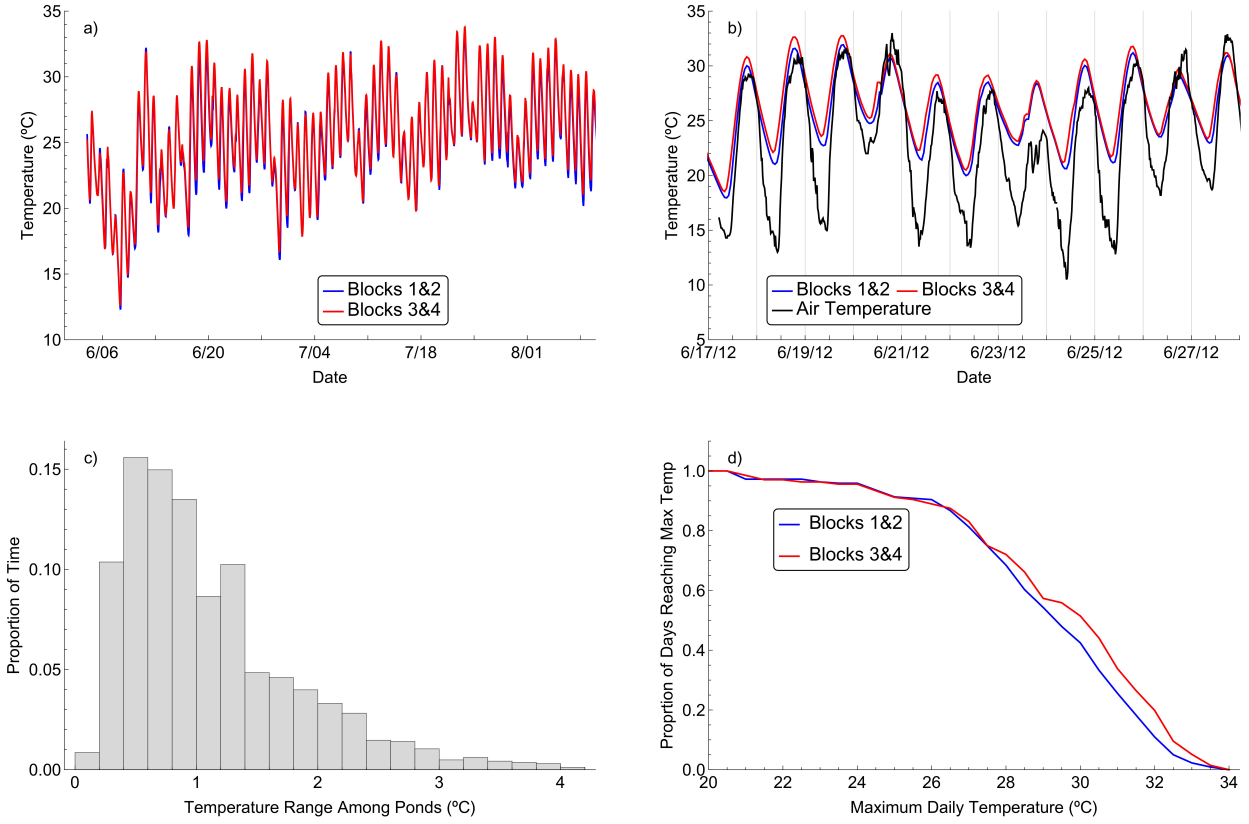

Supporting Information Fig. S6. Summary of temperature measurements from the ponds. Mean temperature in blocks 1&2 and blocks 3&4 over the course of the experiment (a). Comparison of pond temperature and air temperature during a representative time period (b). Vertical gridlines are at 0:00 local time (midnight). Distribution of maximum temperature range observed among the ponds that contained temperature loggers (c). Proportion of days during the experiment that reached or exceeded maximum temperatures in blocks 1&2 and blocks 3&4 (d).

Growth rate estimates. The exponential growth rate for each pond was estimated from the increase in biomass between inoculation (~1 mg L^{-1}) and the first two weeks of the experiment using the following equation:

$$growth\ rate = \frac{\log\left(\frac{biomass_{t2}}{biomass_{t1}}\right)}{t2 - t1}$$

where $biomass_{t1}$ represents biomass at time 1 (mg L^{-1}), $biomass_{t2}$ represents biomass at a subsequent time point (mg L^{-1}), and t2 - t1 is the number of days between measurements. The maximum observed growth rates are displayed in Fig. S7. We tested for differences among species compositions using a mixed-effects linear model with species composition as a fixed effect and block as a random effect. This model identified significant differences in maximum growth rate among the species compositions ($F_{10,63}$=5.58, $p<10^{-4}$). Post-hoc tests showed two species compositions with poor growth rates: species composition A had significantly lower growth rates than F, AB, AF, and BF and species composition AD had significantly lower growth rate than B, F, AB, AF, BD, and BF.

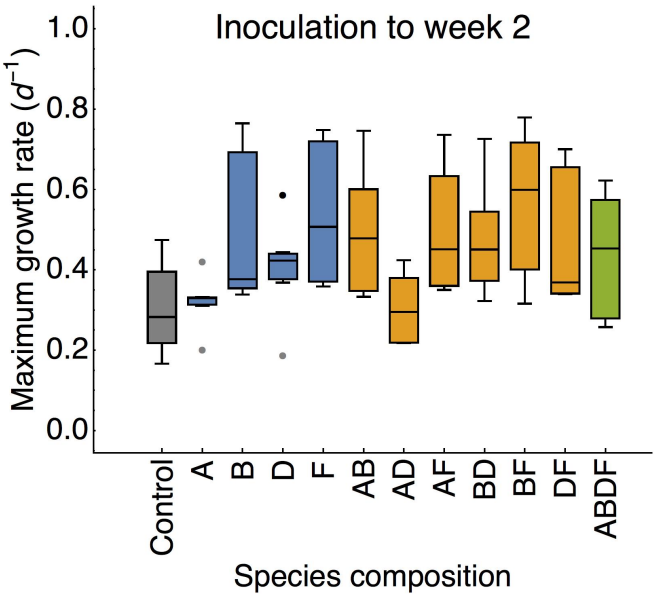

Supporting Information Fig. S7. Box-whisker charts showing the maximum growth rate of each species composition, between the time of inoculation and week 2 of the experiment.

Styling and species codes are described in Fig. 1.

Supplemental References

American Public Health Association. (1995). *Standard methods for the examination of water and wastewater: Including bottom sediments and sludges* (20th ed.). New York: American Public Health Association.

Hietala, D. C., Koss, C. K., Narwani, A., Lashaway, A. R., Godwin, C. M., Cardinale, B. J., & Savage, P. E. (2017). Influence of biodiversity, biochemical composition, and species identity on the quality of biomass and biocrude oil produced via hydrothermal liquefaction. *Algal Research, 26*, 203-214.

Narwani, A., Lashaway, A. R., Hietala, D. C., Savage, P. E., & Cardinale, B. J. (2016). Power of plankton: Effects of algal biodiversity on biocrude production and stability. *Environmental Science & Technology, 50*(23), 13142-13150.

Ringuet, S., Sassano, L., & Johnson, Z. I. (2011). A suite of microplate reader-based colorimetric methods to quantify ammonium, nitrate, orthophosphate and silicate concentrations for aquatic nutrient monitoring. *Journal of Environmental Monitoring, 13*(2), 370-376.

Wetzel, R. G. (2001). *Limnology : Lake and river ecosystems* (3rd ed.). San Diego: Academic Press.

Wetzel, R. G., & Likens, G. E. (2000). *Limnological analyses* (3rd ed.). New York: Springer.